

PAPER • OPEN ACCESS

InSAR monitoring data to assess building response to deep excavations

To cite this article: S Ritter and R Frauenfelder 2021 *IOP Conf. Ser.: Earth Environ. Sci.* **710** 012036

View the [article online](#) for updates and enhancements.

You may also like

- [Impacts of 25 years of groundwater extraction on subsidence in the Mekong delta, Vietnam](#)
P S J Minderhoud, G Erkens, V H Pham et al.
- [Research on Block Adjustment of Airborne InSAR Images](#)
Yue Xijuan, Han Chunming, Dou Changyong et al.
- [Assessment of hydrologic connectivity in an ungauged wetland with InSAR observations](#)
Fernando Jaramillo, Ian Brown, Pascal Castellazzi et al.



The Electrochemical Society
Advancing solid state & electrochemical science & technology

242nd ECS Meeting

Oct 9 – 13, 2022 • Atlanta, GA, US

Abstract submission deadline: April 8, 2022

Connect. Engage. Champion. Empower. Accelerate.

MOVE SCIENCE FORWARD



Submit your abstract



InSAR monitoring data to assess building response to deep excavations

S Ritter¹ and R Frauenfelder¹

¹ Norwegian Geotechnical Institute (NGI), Sognsveien 72, 0855 Oslo, Norway

stefan.ritter@ngi.no

Abstract. Recently, there has been growing interest to use Interferometric Synthetic Aperture Radar (InSAR) to quantify ground displacements. While InSAR can well determine the area and magnitude of subsidence, very little attention has been paid to explore InSAR measurements to assess the building response adjacent to geotechnical works (e.g., deep excavations, tunnelling). Specifically, few studies have investigated the ability of using InSAR to derive widely accepted building deformation parameters including angular distortion and horizontal strain. On the other hand, geotechnical engineers generally use traditional monitoring data to assess the behaviour of existing structures adjacent to excavations, but often only spatially and temporally limited monitoring data exist to reliably evaluate the governing mechanisms. This contribution follows a case study approach to explore the value of InSAR to quantify the effects of excavation-induced settlements on buildings. Conventional monitoring data of structures adjacent to excavation works for a construction project in Oslo, Norway, are compared to InSAR measurements from satellites with different spatial resolutions and from two different processing methods. Differences between displacements obtained from these different InSAR monitoring datasets and their practical implementation are discussed. Building deformations and respective damage categories are then quantified using a methodology that combines both InSAR and inclinometer measurements. As expected, it was found that high resolution InSAR measurements are more reliable when assessing the building response to excavation works.

1. Introduction

The construction of deep excavations in soft soils can affect neighbouring structures. During construction works, excavation-induced displacements are generally monitored using precise levelling and total stations. Recently, the feasibility of the Interferometric Synthetic Aperture Radar (InSAR) monitoring technique for such type of monitoring has been explored. Some studies used InSAR to obtain the 'influence area' of excavation works for large infrastructure projects (e.g., [1]). In others, InSAR data was recently used to investigate building deformations caused by tunnelling [2,3].

So far, little attention has been paid to explore this technique to monitor building response to deep excavations. Specifically, only a few studies (e.g., [4]) used InSAR to assess the structural behaviour of buildings adjacent to deep excavations. This shortcoming is likely due to the variability in the soil displacement profiles compared to tunnelling. Vital sources of this complexity are the soil type, the

applied support techniques (e.g., wall type and lateral support system) and the excavation method. For this reason, a considerable amount of literature has been published that propose deep excavation-induced settlement profiles which differ in shape and extension.

Methods to assess the potential risk of excavation-induced building damage are often based on greenfield conditions where buildings are not present. These methods provide a first mean to screen many buildings but neglect the interaction between the building and the soil, which often leads to conservative estimates. Structural monitoring data of buildings nearby deep excavations may allow to quantify the building response to deep excavations, and to provide assessment methods that account for soil-structure interaction effects. However, high quality field data is often scarce [5] and the practicability of using widely available monitoring data from InSAR to assess building response to deep excavations has not yet been explored in detail.

This paper uses a case study to discuss the practicability of employing InSAR monitoring data from different satellites to evaluate the risk of excavation-induced damage. Publicly available InSAR results from InSAR Norway (<https://insar.ngu.no/>) and results from own processing of commercial InSAR data is compared to traditional levelling data. Firstly, characteristics of settlements caused by deep excavations are introduced, followed by a discussion of the case study area and the available monitoring datasets. The data processing and procedure used to obtain deformation parameters for single buildings is presented. Computed damage categories affected by the different monitoring techniques are shown and discussed. The paper concludes with a set of practical recommendations to overcome observed limitations with respect to the different InSAR monitoring datasets.

2. Excavation-induced building damage

Subsidence due to excavation works poses a significant risk to adjacent structures. In a first stage, assessment methods often describe the excavation-induced ground displacements as if buildings were not present (i.e., greenfield conditions). For deep excavations, Lee et al. [6] presented the following vertical and horizontal settlement curves:

$$S_v(x) = S_{v,\max} e^{\left(0.5 - 0.5\left(\frac{1+2x}{W}\right)^2\right)} \quad (1)$$

$$S_h(x) = \beta \left(1 + \frac{2x}{W}\right) S_v(x) \quad (2)$$

where x is the horizontal distance from the support wall, S_v and S_h the vertical and horizontal soil displacement, β the ratio of S_v to S_h and W the trough width parameter. The maximum vertical soil displacement, $S_{v,\max}$, is often defined to be equal to the maximum horizontal wall displacement, $u_{h,\max}$. According to Lee et al. [6], β can be assumed to be 0.5 for diaphragm walls and 1.0 for sheet pile walls. Caspe [7] related W to the excavation depth, H , the influence depth below the excavation, H_d , and the soil friction angle, φ' , which can be expressed as:

$$W = (H + H_d) \tan\left(45 - \frac{\varphi'}{2}\right) \quad (3)$$

with $H_d = 0.5 B \tan\left(45 - \frac{\varphi'}{2}\right)$ for soils with $\varphi' > 0$ and $H_d = B$ applies for cohesive soils where B is the excavation width. Figure 1 depicts these settlement profiles which reasonably well characterize cantilever type wall deformations. Displacement profiles for other deflected shapes of the support wall are presented in other studies (e.g., [8]).

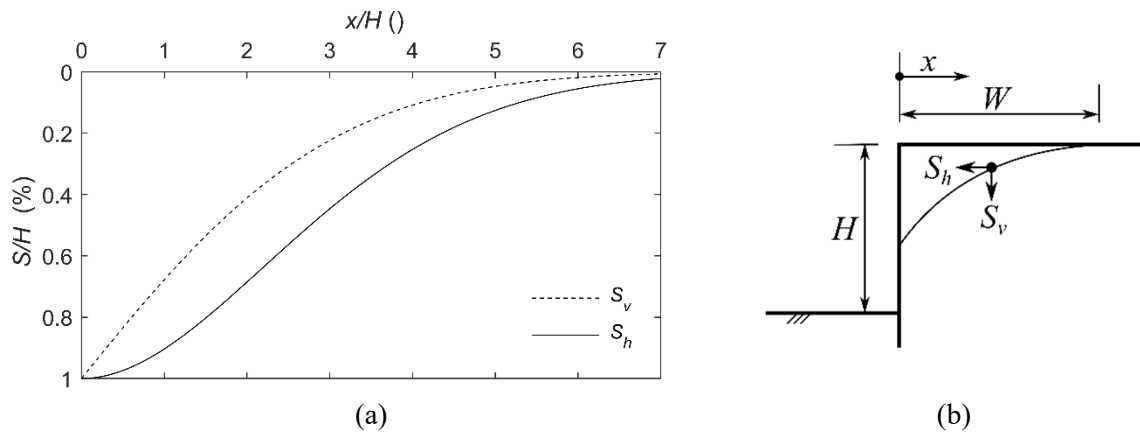


Figure 1. Ground movements caused by deep excavations: (a) vertical, S_v , and horizontal, S_h , settlement profiles and (b) adopted sign convention.

In the next stage, these greenfield profiles are imposed to a simplified building model and deformations parameters are evaluated, as shown in figure 2. Widely used parameters are the so-called angular distortion, β_{ang} , and the lateral strain, $\varepsilon_{lat} = \Delta L/L$, which can be related to tensile building strains and related damage [9]. Note that the β_{ang} is often approximated as the first derivative of the vertical displacement profile (i.e. slope), which neglects any rigid body rotation, an approximation also applied in this paper. Figure 3 shows the relationship between building damage, β_{ang} and ε_{lat} . Following Son and Cording [9], the maximum principal building tensile strain can be written as:

$$\varepsilon_p = \varepsilon_{lat} \cos(\theta_{max})^2 + \beta_{ang} \sin(\theta_{max}) \cos(\theta_{max}) \quad (4)$$

$$\tan(2\theta_{max}) = \frac{\beta_{ang}}{\varepsilon_{lat}} \quad (5)$$

where θ_{\max} defines the cracking direction and the angle between the vertical and the plan on which ε_p acts.

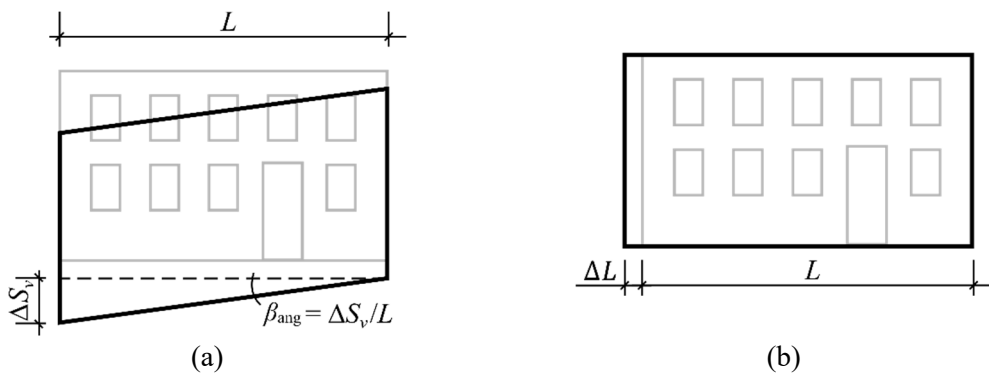


Figure 2. Building deformation parameters: (a) angular distortion, β_{ang} , and (b) lateral strain, ε_{lat} . Grey lines indicate the undeformed building.

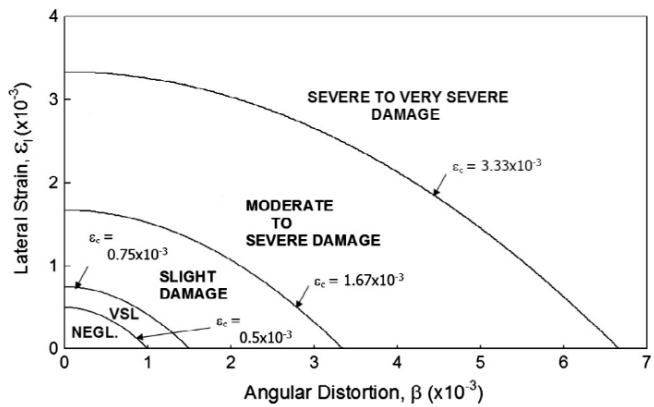


Figure 3. Damage category chart according to Son and Cording [8].

3. Case study area

This section provides a brief overview of the case study area, which is a deep excavation site for the Follo Line project in Oslo, Norway. Figure 4 shows a plan view of the case study area and indicates the neighbouring structures. Additionally, the location of an inclinometer is indicated which monitored the deformation of the support wall.

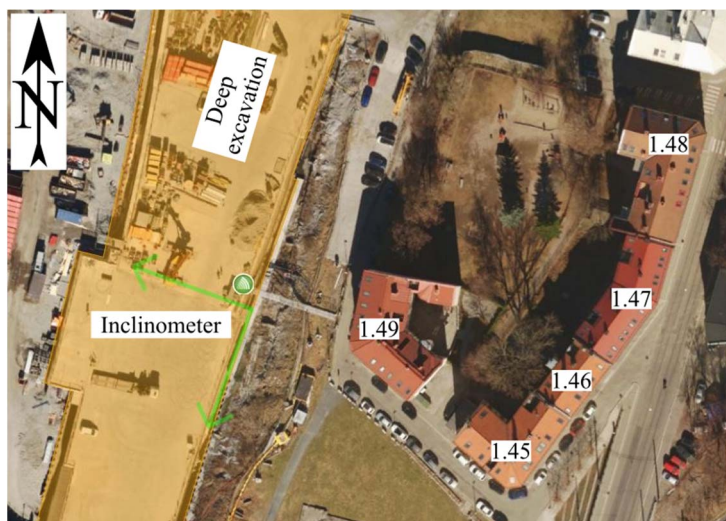


Figure 4. Case study area showing the deep excavation site, adjacent buildings and the inclinometer position (Picture source: Cautus Web, <http://www.monitorering.no/> © Cautus Geo).

Figure 5 depicts the excavation support system including sheet pile walls, jet grouting columns, lime-cement stabilised soil layers and diagonal props as lateral wall support. Micropiles to bedrock were used to support the final concrete structure. The sheet pile wall facing the surrounding buildings was designed with a length of 24 m. Note that the ground profile increases towards the adjacent structures. The average excavation depth was approximately 6 m and the excavation width approximately 40 m.

The subsurface conditions in the case study area are typical for Oslo. A 1 to 5 m thick layer of historical anthropogenic fill material is followed by a soft clay layer with a thickness between 15 to 40 m. The depth to bedrock varies between the isolines -17 m and -35 m. The water level of the lowest aquifer is at a variable depth between -6.5 and -9 m.

Inclinometers were installed along the excavation to monitor the displacement of the sheet pile wall during the construction phase. The lateral displacements of an inclinometer in the case study area (location given in figure 4) are given in figure 6. The data was analysed by assuming that the deep end of the inclinometer is not affected by excavation-induced displacements. This is clearly a simplification considering the notable rotation of the deep end of the inclinometer. However, further monitoring data was not collected to obtain a possible horizontal movement of the inclinometer toe.

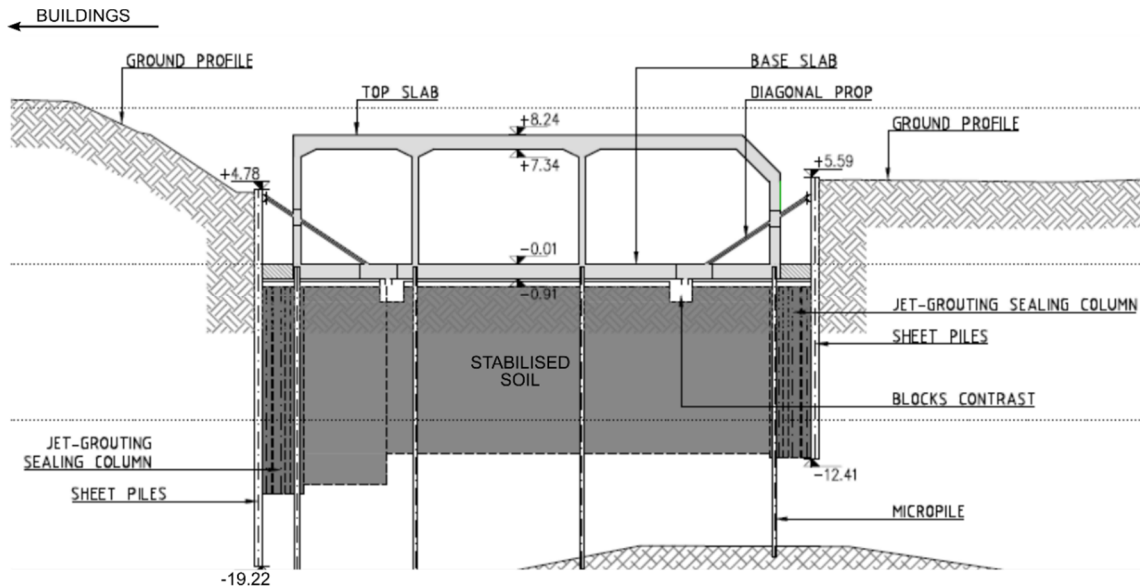


Figure 5. Excavation support system in case study area (Picture source: Jernbaneverket, Document ID: UOS-10-A-52002).

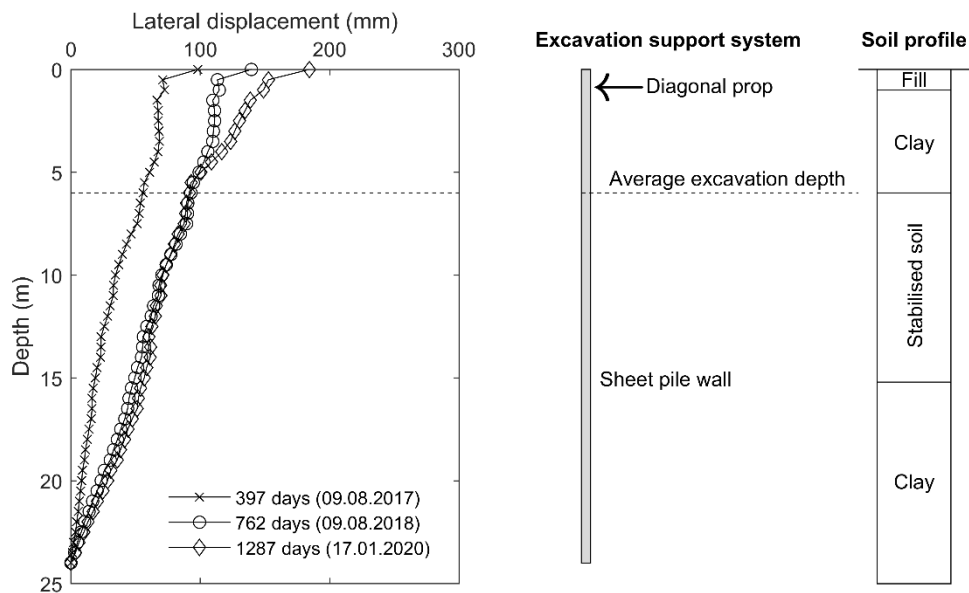


Figure 6. Lateral displacements at inclinometer location in case study area (see figure 4) and overview of excavation support system and soil profile.

The lateral displacements in figure 6 are shown for three different dates after the first inclinometer reading. The lateral displacements gradually developed and were largest at the surface. The observed cantilever type of displacement can be explained by the chosen excavation sequence. The inclined props (figure 5) were installed after first excavation works to the depth of the base slab were conducted. A more detailed discussion of the performance of the excavation support system and the ground response is not the focus of this paper.

4. Monitoring Dataset

The effect of the excavation works on the surrounding infrastructure was monitored using both ground-based measurements (i.e., precise levelling) and satellite-based InSAR. Three different InSAR datasets with different ground resolutions were explored, as shown in figure 7. These are: (1) Sentinel-1 with a ground resolution of approximately 5 x 20 m (5 m in East-West and 20 m in North-South direction), (2) Radarsat-2 Fine Mode with an approximate ground resolution of 7 x 7 m, and (3) TerraSAR-X Staring Spotlight with an approximate ground resolution of 0.6 x 0.25 m. The Sentinel-1-based InSAR results were downloaded in June 2019, from the publicly available "InSAR Norway" service (<https://insar.ngu.no/>). Only one of four available geometries was used, i.e. the Sentinel-1 Descending 1 geometry (for details, please consult <https://www.ngu.no/en/topic/about-mapping-service>). For the Radarsat-2 and TerraSAR-X data, the SARscape™ software was used for data processing. The Radarsat-2 data were processed using the Permanent Scatter (PS) workflow, whereas the TerraSAR-X data was processed with both the PS and the Small Baseline Subset (SBAS) workflows.

Ground-based monitoring in the form of precise levelling was conducted to obtain the vertical building displacements. A base line reading was obtained in October 2011. Throughout the construction period further measurements were conducted at monthly intervals. The traditional monitoring data represents the benchmark data for comparison with the InSAR measurements. In the following, the methodology used to determine building damage categories is discussed, after which the results obtained with the different monitoring datasets are discussed.

5. Methodology

To determine whether InSAR can reliably be used to assess the risk of building damage, damage categories were derived from InSAR measurements and compared to damage categories based on traditional monitoring data. The first step in this process was to obtain monitoring data for each asset. Only monitoring points located within or on the building perimeter and data between June 1, 2016 and August 9, 2018 were considered. For Radarsat-2 and TerraSAR-X, vertical deformation was computed directly during in-house processing. The results in "InSAR Norge" are available in Line-of-sight (LOS) only. Therefore, the Sentinel-1 LOS displacement measurements were converted to vertical deformations by using:

$$S_v = \frac{LOS}{\cos(\theta)} \quad (6)$$

where θ is the incidence angle in each considered data point. Using equation (6) assumes that most of the displacements occur vertically, which is a notable simplification and further discussed below.

The building shape was simplified by transferring its geometry onto a theoretical building length, L_{bldg} , perpendicular to the deep excavation, as shown in figure 8. This approach is clearly also a simplification, but allows one to equally consider all building monitoring points along a section perpendicular to the excavation wall. Subsequently, each monitoring dataset was fitted with the theoretical vertical settlement profile, as presented in equation (1). To make use of the available inclinometer data, $S_{v,max}$ was constrained to the maximal lateral wall displacement (-139.5 mm for August 9, 2019, figure 6). The horizontal displacement profile for each asset and each monitoring dataset was obtained by adopting the relation between S_h and S_v , as stated in equation (2). Subsequently, the building deformation parameters β_{ang} and ε_{lat} were derived for each building and respective damage classes were calculated.

6. Results and discussion

To compare the differences between the analysed monitoring datasets, the methodology described above was carried out. For each single building, the data within a building polygon was considered, as exemplified in figure 9a for building 1.47. As expected, this figure indicates that the results from the higher-resolution InSAR data (i.e., TerraSAR-X) provide a considerably greater amount of monitoring points per asset. By contrast, only a limited number of data points were obtained for the coarser resolution InSAR datasets (i.e., Sentinel-1 and Radarsat-2). For the buildings 1-45 and 1-49, Radarsat-

2 measurements could not be obtained (figure 7b). This implies that a detailed analysis of building response to excavation works can generally only be carried out with high resolution InSAR data.

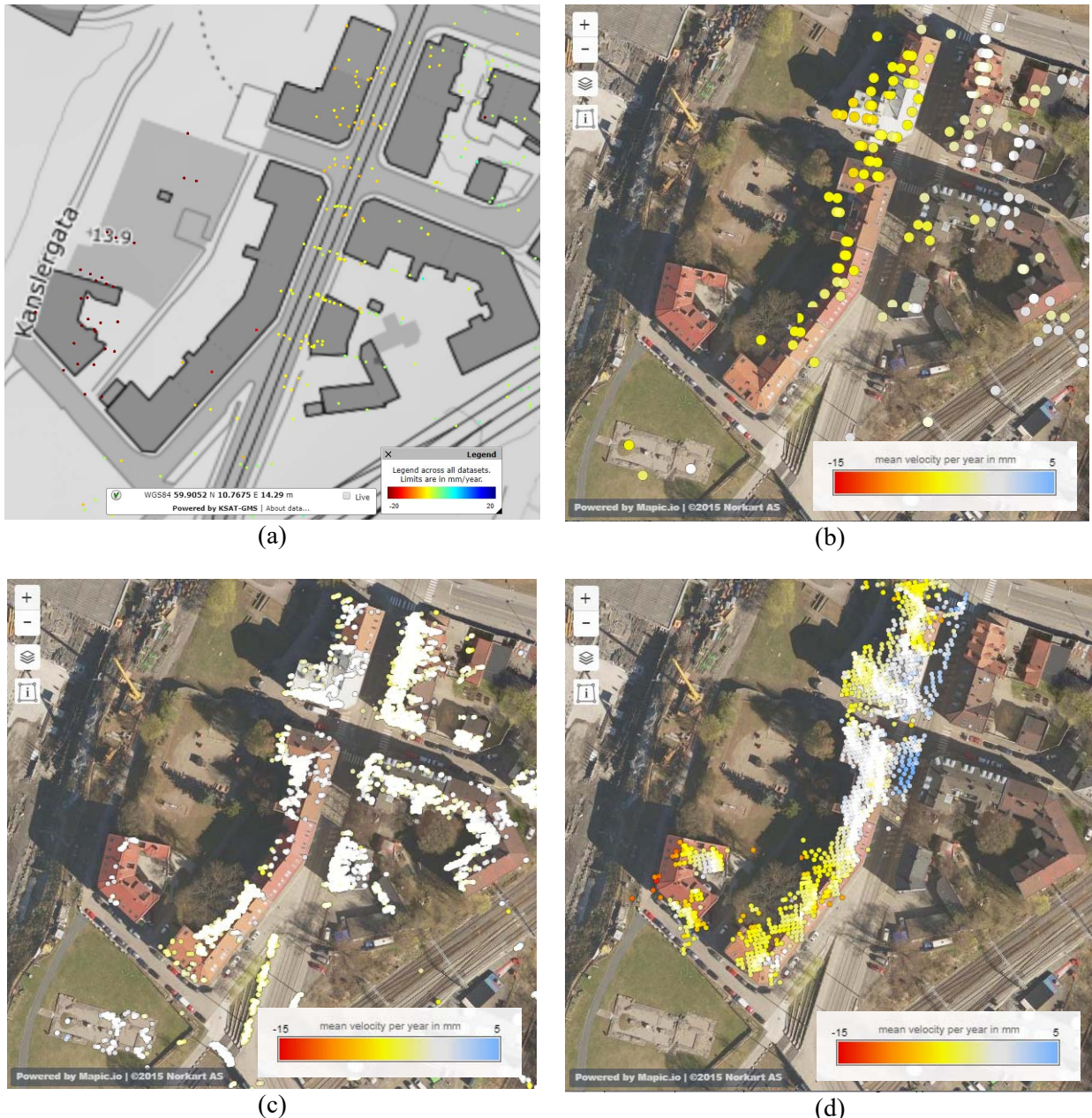


Figure 7. Settlement velocities in case study area: (a) June 2016 to October 2018, based on Sentinel-1 data (resolution: ca. 5 x 20 m). Source: InSAR Norway, insar.ngu.no; (b) April 2014 to December 2019, based on Radarsat-2 data (resolution: ca. 7 x 7 m). Raw data source: Radarsat-2 Fine Mode data 2014–2019 (Copyright © MDA/NSC/KSAT 2014–2019); (c) April 2014 to August 2018, based on TerraSAR-X (resolution: 0.6 x 0.25 m) and processed with PS workflow. Raw data source: TerraSAR-X staring spotlight data 2014–2018 (Copyright © 2014–2018 DLR, Distribution Airbus DS/Infoterra GmbH); (d) April 2014 to August 2018, based on TerraSAR-X (resolution: 0.6 x 0.25 m) and processed with Small Baseline Subset (SBAS) workflow. Raw data source as in (c).

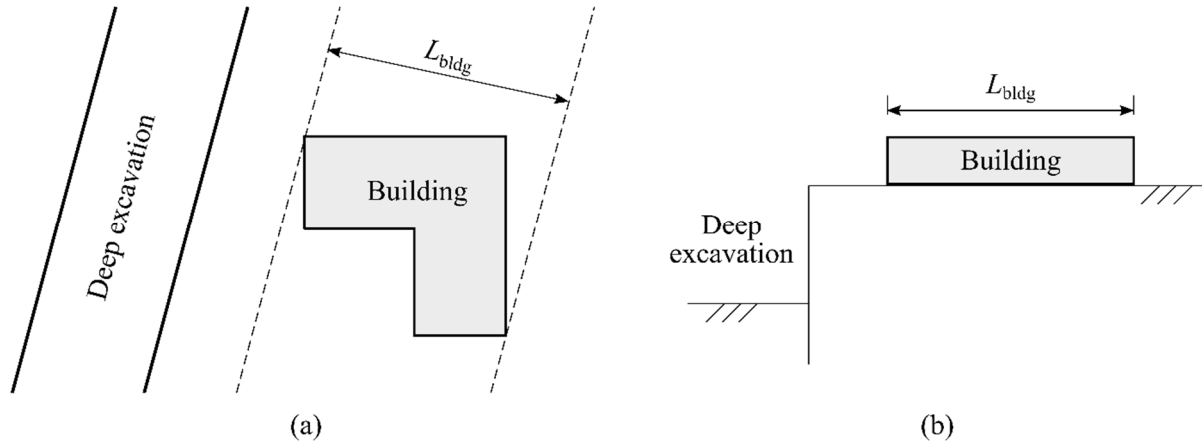


Figure 8. Theoretical building length, L_{bldg} , estimation: (a) plan view and (b) transection.

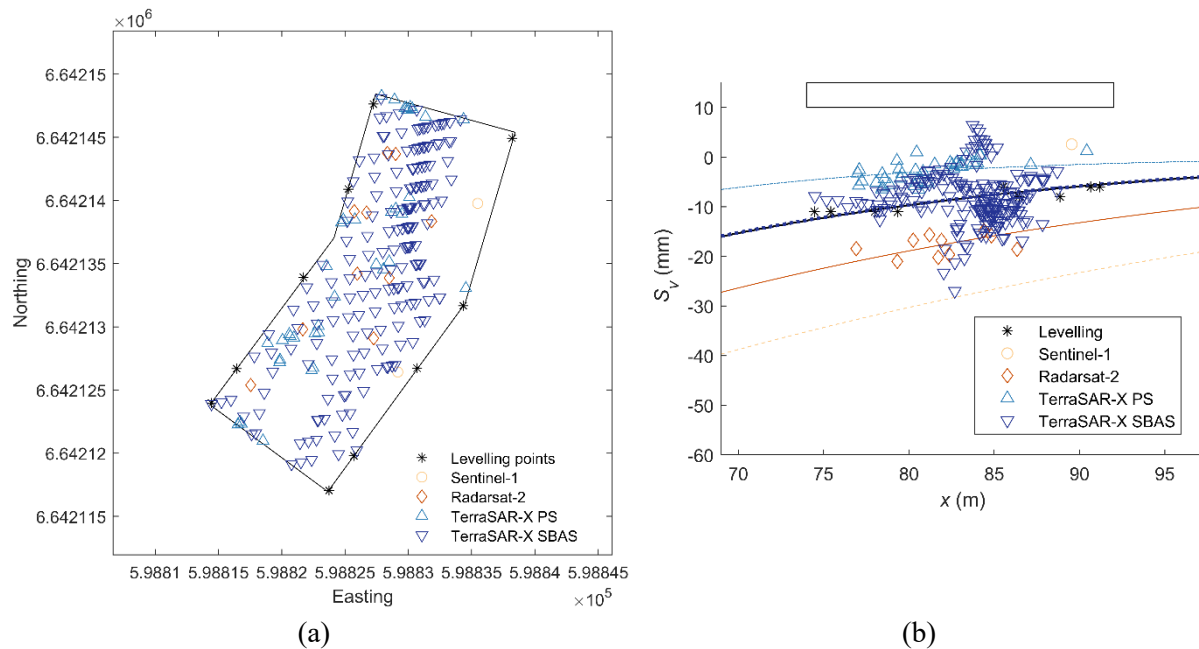


Figure 9. Monitoring data for building 1.47: (a) different monitoring datasets and (b) transection and curve fitting. Colours indicate curves fitted to monitoring data. Curves fitted to levelling and TerraSAR-X SBAS data are almost identical.

Contrary to the PS results, figure 9b indicates that the SBAS vertical displacements derived from the TerraSAR-X data are in good agreement with the levelling data. Although – from experience – unwrapping errors can exist also in SBAS results, it is generally found that the SBAS processing is less sensitive to sudden changes in the displacement rate, compared to the PS processing.

A further aspect to consider when comparing the measurement series is their acquisition geometry. While the Sentinel-1 measurements were performed in descending geometry, both the Radarsat-2 and the TerraSAR-X measurements were derived in ascending geometry. In descending geometry, vertical displacements for measurement points that move horizontally to the West (i.e., towards the excavation, see figure 4) are generally overestimated.

The curves fitted to the vertical displacement data were subsequently used to derive horizontal displacement profiles and building deformation parameters (i.e., β_{ang} and ε_{lat}). Maximum principal

building tensile strains (equation 4) were calculated for each asset from each monitoring dataset. Figure 10 summarises the obtained results and relates them to widely accepted building damage categories. Although the displacements measured by the different monitoring techniques differed, as mentioned above, the building damage categories are in fair agreement. This encouraging finding is a direct result of incorporating the available inclinometer data (see section 5) which defines the shape of the fitted curves.

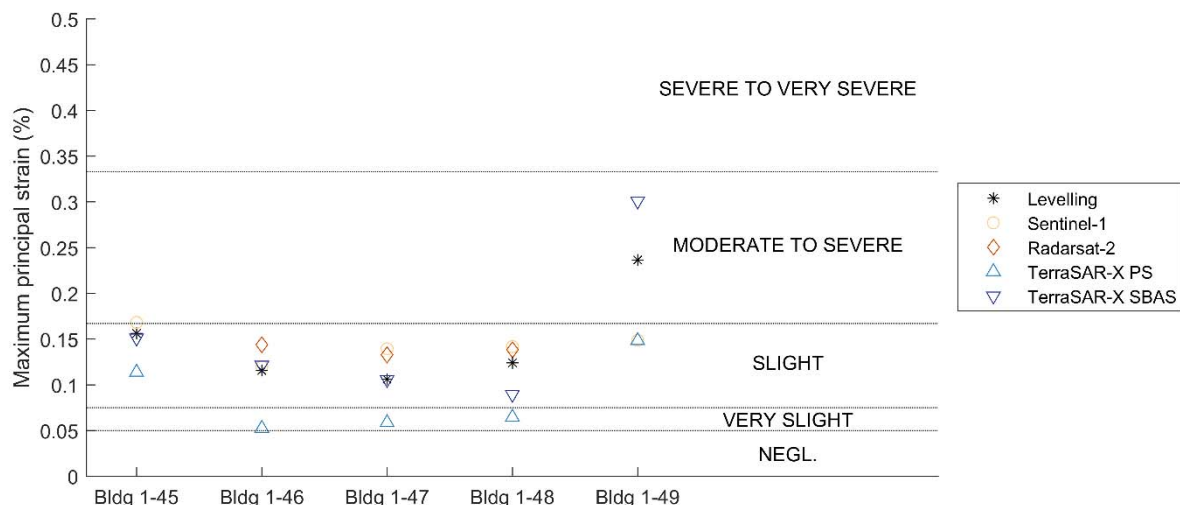


Figure 10. Building damage categories based on different monitoring datasets.

For all the buildings analysed, the TerraSAR-X SBAS measurements resulted in the identical damage categories as the precise levelling data. By contrast, the TerraSAR-X PS data seems to underestimate the damage categories, as can be seen in figure 10. The Sentinel-1 and Radarsat-2 were in good agreement with the precise levelling data. However, the Sentinel-1 data underestimated the building damage category for building 1-49 (figure 10). Additional studies using a wider set of case studies will be required to generalise these findings.

7. Conclusions

This contribution set out to analyse the practicability of InSAR in the assessment of building response to excavation-induced displacements. Results based on different InSAR datasets and from two different processing approaches were compared to precise levelling data. In our case study, significant differences in the magnitude of the InSAR-derived settlement measurements were observed. Thanks to the incorporation of available inclinometer data, these differences did not linearly percolate into the derivation of the building response parameters. This is a promising finding; yet, our results also show that the interpretation of excavation-induced building displacements based on solely InSAR still needs to be carried out with extreme caution. This is particularly true for low resolution InSAR data.

This study has further shown that considering theoretical displacement profiles caused by deep excavations in combination with measured wall displacements can result in building response assessments that are in line with precise levelling data. Specifically, building damage categories based on TerraSAR-X SBAS measurements were identical with the ones from ground-based monitoring. Our findings suggest that the quality of the InSAR measurements can be refined by accounting for phase unwrapping and by carrying out decomposition into vertical and horizontal displacement components.

The major limitation of this contribution is that only a single study area could be investigated. A natural progression of this work would be to analyse further assets.

Acknowledgements

The authors are grateful to the Norwegian Space Centre (contract JOP.05.19.2) and the Norwegian Research Council (through its annual base funding to NGI) for supporting this research. Further, the authors acknowledge the Norwegian National Rail Administration (Bane NOR) for giving permission to publish the results of this case study. Finally, the authors thank Jonas Forsmo for helping with data collection while being a summer student at NGI in 2019.

References

- [1] Frauenfelder R, Vöge M, Pfaffhuber A A., Hauser C, Dehli G and Syversen F 2019. Settlement monitoring using space-borne radar interferometry, in the context of large infrastructure projects In XVII ECSMGE 2019.
- [2] Giardina G, Milillo P, DeJong M J, Perissin D and Milillo G 2019. Evaluation of InSAR monitoring data for post-tunnelling settlement damage assessment. *Structural Control and Health Monitoring*, **26**(2), 1-19.
- [3] Milillo P, Giardina G., DeJong M J, Perissin D and Milillo G 2018. Multi-temporal InSAR structural damage assessment: The London crossrail case study. *Remote Sensing*, **10**(2), 1-11.
- [4] Korff M and Maccabiani J. 2017. Building damage related to Amsterdam subway: Comparison of traditional monitoring with satellite monitoring results. In EURO:TUN 2017, Innsbruck, Austria.
- [5] DeJong M J, Giardina G, Chalmers B, Lazarus D, Ashworth D and Mair R J 2019. Impact of the Crossrail tunnelling project on masonry buildings with shallow foundations. *Proceedings of the Institution of Civil Engineers - Geotechnical Engineering*, **172**(5), 402-416.
- [6] Lee S J, Song T W, Lee Y S, Song Y H and Kim I K 2007. A case study of building damage risk assessment due to the multi-propped deep excavation in deep soft soil. In 4th Int. In Conf. Soft Soil Eng. Vancouver, London, Taylor Francis.
- [7] Caspe M S 1966. Surface Settlement Adjacent to Braced Open Cuts. *Journal of the Soil Mechanics and Foundations Division*, ASCE, **92**(4), 51-59.
- [8] Clough G W and O'Rourke T D 1990. Construction Induced Movements of Insitu Walls. In Design and Performance of Earth Retaining Structures, New York, USA, 439-470.
- [9] Son M and Cording E J 2005. Estimation of building damage due to excavation-induced ground movements. *Journal of geotechnical and geoenvironmental engineering*, **131**(2), 162-177.